LETTER

ACS chemical biology

Accurate Targeting of Activated Macrophages Based on Synergistic Activation of Functional Molecules Uptake by Scavenger Receptor and Matrix Metalloproteinase

Hideyuki Suzuki[†], Moritoshi Sato[‡,§], and Yoshio Umezawa[†,‖,*]

[†]Department of Chemistry, School of Science, The University of Tokyo, Hongo, Bunkyo-ku, Tokyo 113-0033, Japan, [‡]Graduate School of Arts and Sciences, The University of Tokyo, Komaba, Meguro-ku, Tokyo 153-8902, Japan, and [§]PRESTO, Japan Science and Technology Agency, Sanbancho, Chiyoda-ku, Tokyo 102-0075, Japan, [‖]Present address: Research Institute of Pharmaceutical Sciences, Musashino University, 1-1-20 Shinmachi, Nishitokyo-shi, Tokyo 202-8585, Japan.

Controlled delivery of compounds to particular cell types is a key process for both precise diagnostic imaging and risk-free therapies of diseases (*1–3*). This process is known as cell targeting. Most of existing techniques for the cell targeting are based on the development of molecules, as represented by antibodies (*4*) or peptide ligands (*5, 6*), which bind to characteristic surface markers of disease cells, such as receptor proteins and glycoproteins. However, this approach does not always give satisfactory results because the characteristic surface markers, which are expressed in disease cells but not in healthy cells, are not always available. In many cases, no significant differences in the expression of surface proteins are found between disease cells and healthy cells. Therefore, the existing methods based on only the recognition of the surface markers have limitations in specific targeting of disease cells.

Macrophage is an immune cell that plays a key role in all the phases of atherosclerosis from its initiation to progression (*7*). In atherosclerotic lesions, aberrant accumulation of macrophages, which are differentiated from circulating blood monocytes, is observed. The macrophages in atherosclerotic lesions, known as activated macrophages, express scavenger receptors (SR) responsible for the clearance of pathogenic lipoproteins, such as oxidized low-density lipoprotein (oxLDL), in atherosclerotic lesions (*8*). However, macrophages in normal tissues, namely, resting macrophages, also express SR (*8, 9*). There is mounting evidence that, in addition to the increased expression of cell surface markers, secretion of proteases is often promoted when healthy cells become disease cells, like tumor cells and activated macrophages (*10, 11*). In the case of activated macrophages, the expression and secretion of an activated form of collagen-degrading enzyme, matrix metalloproteinase-9 (MMP-9) (*10, 12*), is remarkably promoted, in addition to the expression of SR. Activated MMP-9 degrades extracellular matrix and weakens physical strength of atherosclerotic lesions (*13*). The resulting rupture of atherosclerotic lesions causes the acute onset of cardiac and brain infarction. On the other hand, resting macrophages in normal tissues do not express the activated form of MMP-9 to a significant extent. In the present study, we develop a molecular probe that binds to SR of macrophages only when the probe is cleaved by MMP-9 secreted from macrophages. This synergistic activation by SR and MMP-9 of the uptake of the probe into cells allowed accurate targeting of activated macrophages expressing both SR and MMP-9, without misincorporation into resting macrophages having only SR.

ABSTRACT Specific targeting of disease cells has the potential of far-reaching applications, such as diagnostic imaging and therapies of diseases. Here we describe a novel method for selective targeting of a type of cells among various cell types. Activated macrophages are disease cells related to initiation and progression of atherosclerosis. We developed a molecular probe of which uptake into cells is synergistically activated by scavenger receptor class A type I (SR-AI) and matrix metalloproteinase-9 (MMP-9), which are the marker receptor and the marker protease of atherosclerosis, respectively. We demonstrated that the present targeting probe is selectively incorporated into activated macrophages expressing both SR-AI and the activated form of MMP-9 but not into resting macrophages having only SR-AI. The present approach may provide a powerful tool for cell-specific imaging and therapies.

***Corresponding author,** umezawa@musashino-u.ac.jp.

Received for review November 29, 2007 and accepted May 21, 2008.

Published online July 1, 2008

10.1021/cb800067e CCC: $40.75

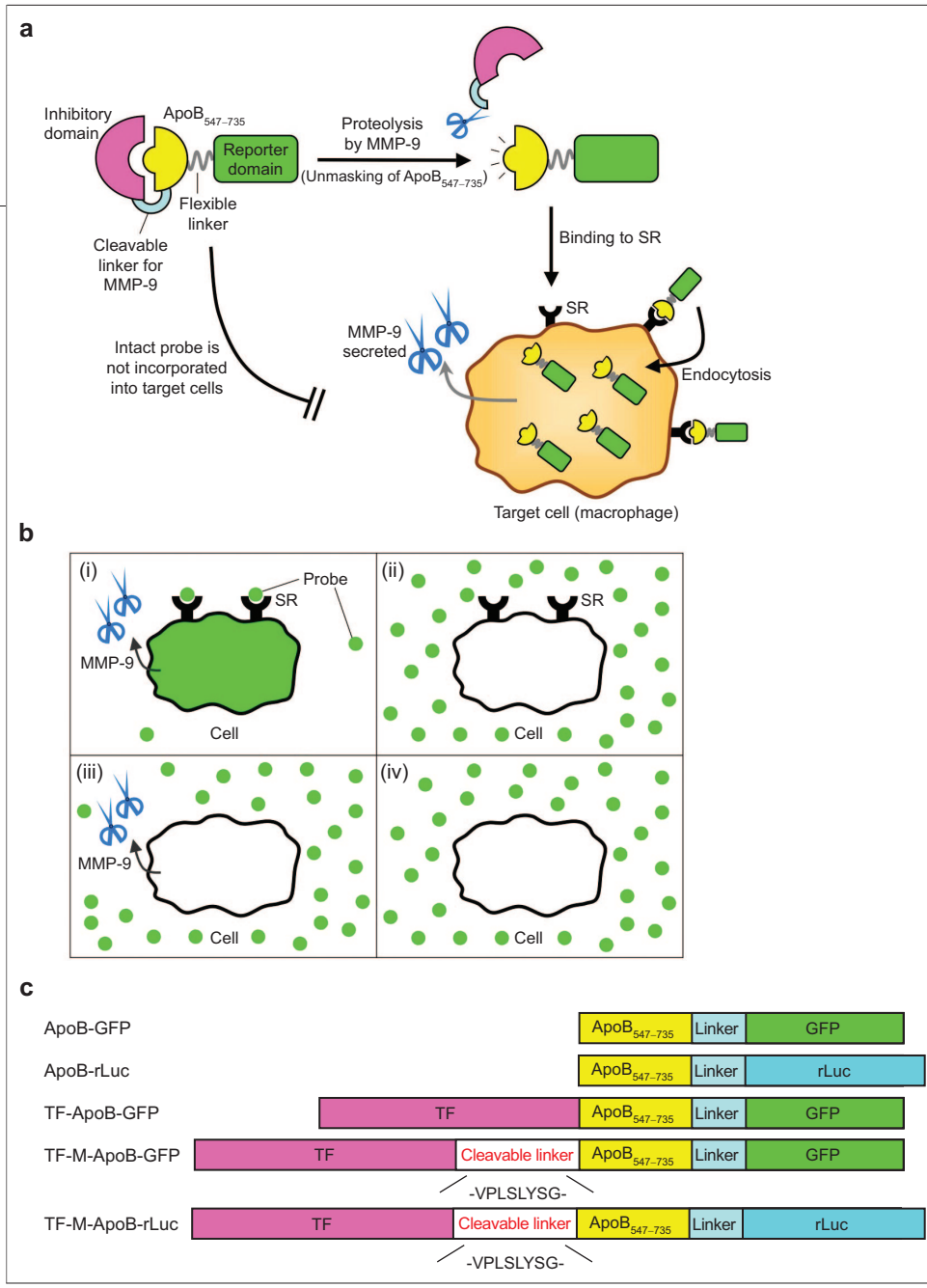

Figure 1. The present probes for accurate targeting of activated macrophages. a) The principle of the present targeting probe, which consists of an inhibitory domain (magenta), a cleavable linker for MMP-9 (light blue), a receptor binding domain ($ApoB_{547-735}$) (yellow), and a reporter domain (green). Once the present targeting probe encounters activated macrophages that express both SR and MMP-9, the inhibitory domain of the probe is dissociated upon cleavage by MMP-9 and then the $ApoB_{547-735}$ domain is exposed to bind to SR. After binding to the receptors, the probe is incorporated into the cells expressing both SR and MMP-9. b) The present targeting probe is incorporated into activated macrophages that express both SR and MMP-9 (i). Cells expressing either SR (ii) or MMP-9 (iii) and cells expressing neither SR nor MMP-9 (iv) do not incorporate the present targeting probe. c) Schematic representations of domain structures of the present probes. Flexible linker sequence, GGSGG.

RESULTS

The present probe is a fusion protein consisting of four domains (Figure 1, panel a), that is, a N-terminal inhibitory domain, followed by a cleavable linker for MMP-9, a receptor-binding domain, and a reporter domain in this order. The receptor-binding domain is derived from a peptide segment of apolipoprotein B ($ApoB_{547-735}$) that binds to SR. We used a chaperon protein of *Escherichia coli* for the inhibitory domain that prevents the interaction between SR and the receptor-binding domain because of its steric hindrance. This inhibitory domain of the present probe is connected with the receptor-binding domain through the cleavable linker peptide that is effectively digested by MMP-9. When the linker is cleaved by MMP-9, the inhibitory domain is dissociated from the probe. The receptor-binding domain of the cleaved probe then binds to SR. Therefore, only the cells expressing both SR and the activated form of MMP-9, like activated macrophages, incorporate the cleaved probe through a SR-mediated endocytosis. In contrast, cells that promote the expression of either SR or MMP-9 do not incorporate this probe (Figure 1, panel b). The reporter domain of the present probe, such as green fluorescent protein and luciferase, allows us to detect the incorporation of this probe into the cells with optical readout.

We first describe the peptide sequence that specifically binds to SR expressed in activated macrophages. The oxLDL, which binds to SR, contains apolipoprotein B (ApoB) and lipids, including fatty acid, cholesterol, and triglyceride (*14*). When they bind to oxLDL, the SR recognizes both ApoB and lipid parts of the oxLDL (*15, 16*). We used a core-binding domain of ApoB to SR (*17*) for the receptor binding domain of the present probe. We coupled the core-binding domain of ApoB ($ApoB_{547-735}$) and GFP through a flexible linker, and named the resulting construct ApoB-GFP. We constructed a cDNA encoding ApoB-GFP (Figure 1, panel c). ApoB-GFP was generated in bacteria and purified by affinity chromatography. Purified ApoB-GFP

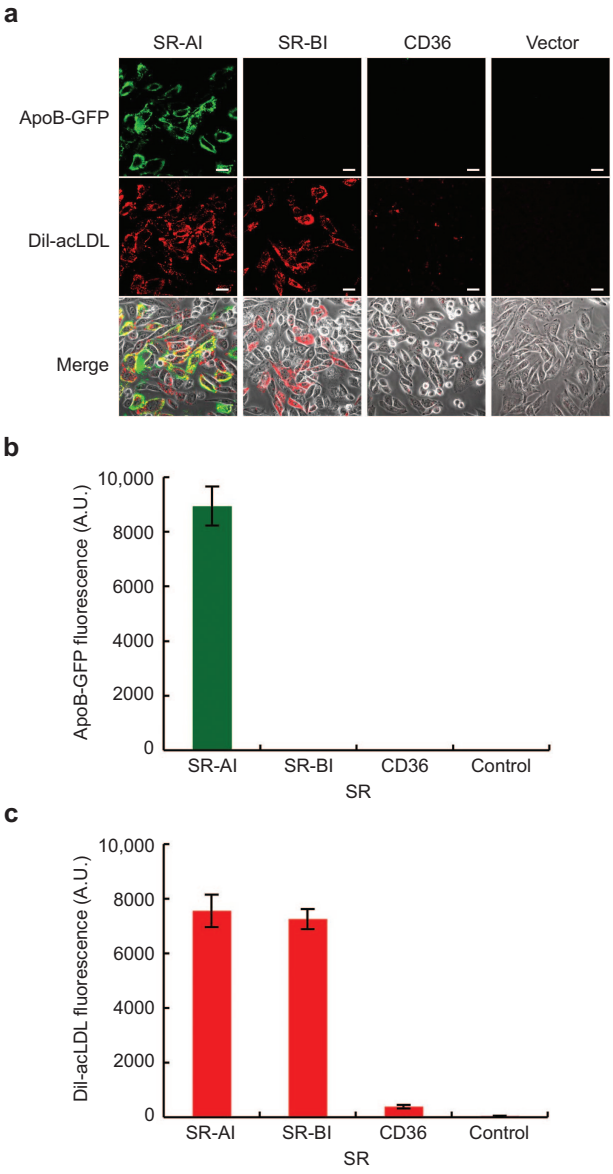

Figure 2. SR-AI-dependent incorporation of ApoB-GFP into cells. CHO-K1 cells were transfected with SR-AI, SR-BI, CD36, or control vector and incubated with 900 nM ApoB-GFP and 10 μg mL^{-1} DiI-acLDL for 3 h. Fluorescence images of cells were acquired by confocal microscopy with a 40× objective (Plan-Neofluar 40×, Carl Zeiss). a) Typical experiments from three independent measurements. Scale bar represents 20 μm. Results shown in panels b and c show fluorescence intensities of b) ApoB-GFP or c) DiI-acLDL inside the cells in panel a. Error bars represent the standard deviation of three independent experiments.

was incubated for 3 h with CHO-K1 cells separately expressing three types of typical SR, scavenger receptor class A type I (SR-AI), scavenger receptor class B type I (SR-BI), and CD36. Green fluorescence was observed within cells expressing SR-AI (Figure 2, panels a and b). On the other hand, there was no detectable green fluorescence within cells expressing SR-BI, CD36, or control vector. The result shows that ApoB-GFP is specifically recognized by SR-AI and incorporated into the cells. In contrast, DiI-labeled acetylated low-density lipoprotein (DiI-acLDL), which mimics oxLDL, was incorporated into both cells expressing SR-AI or SR-BI as reported (*18*) (Figure 2, panels a and c). The expression of CD36 resulted in the incorporation of DiI-acLDL in the cell to a small but significant extent as reported (*18*). Taken together, the core-binding domain of ApoB ($ApoB_{547-735}$) is superior to that of oxLDL or acLDL, having the full-length of ApoB, in terms of selectivity to SR-AI.

We examined whether ApoB-GFP is incorporated into macrophages, which endogenously express SR, such as SR-AI. We used RAW cells derived from mouse macrophages. When we added ApoB-GFP to macrophage-like RAW cells, an increase in the green fluorescence was observed within the cells in a dose-dependent fashion (Figure 3, panels a and b). The increase in the green fluorescence was completely inhibited by pretreating the RAW cells with polyinosinic acid that specifically binds with SR-AI. The result confirms that ApoB-GFP is incorporated into macrophages upon binding with SR-AI.

We show the subcellular distribution of ApoB-GFP incorporated into RAW cells. We incubated RAW cells with both ApoB-GFP and FM 4-64, which stains endosomal membranes. Fluorescence images were acquired by confocal microscopy (Figure 3, panel c). The green fluorescence of ApoB-GFP in the RAW cells colocalized to intracellular endocytotic vesicles stained with FM 4-64. This

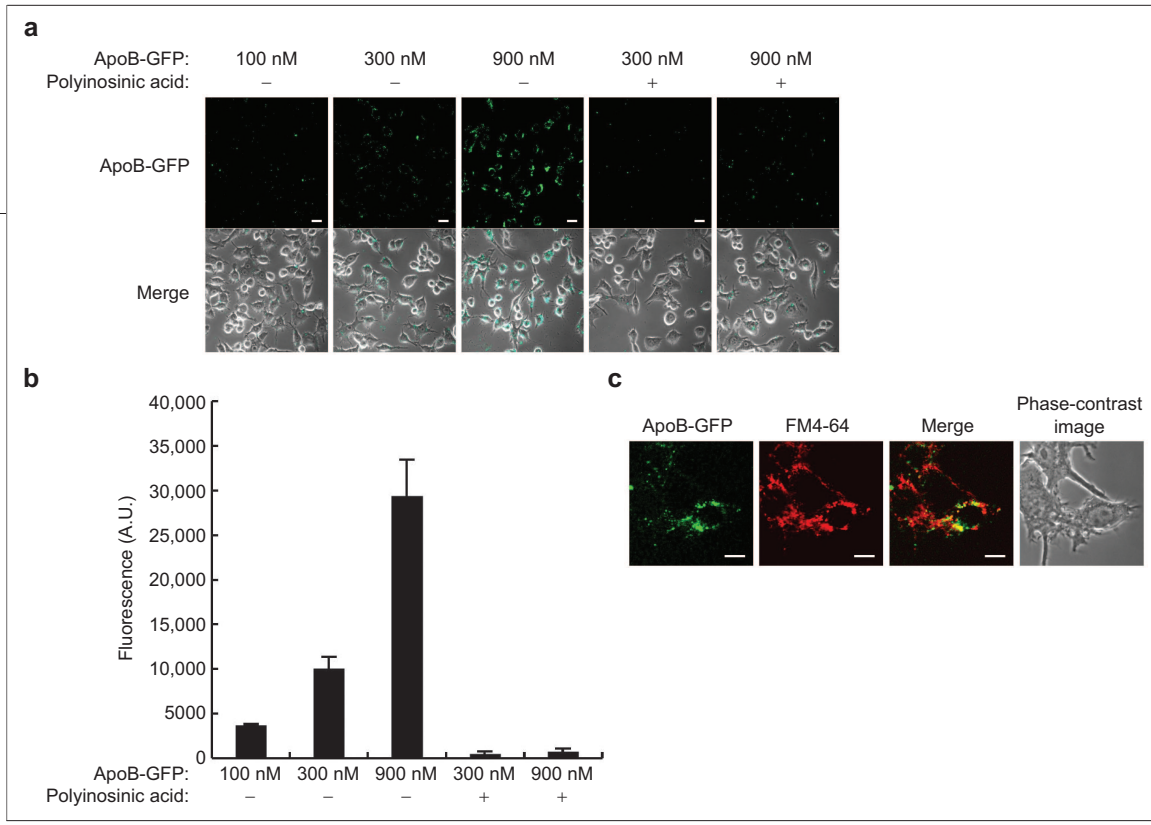

Figure 3. Macrophages incorporate ApoB-GFP. a, b) RAW cells incubated with indicated concentrations of ApoB-GFP for 3 h in the presence or absence of 1 mg mL^{-1} of polyinosinic acid. Fluorescence images of cells were acquired by confocal microscopy with a 40× objective. Panel a represents typical experiments from three independent measurements. Scale bar represents 20 μm. Panel b shows green fluorescence intensities inside the cells in panel a. Error bars represent standard deviation ($n = 3$). c) Subcellular distribution of ApoB-GFP in a RAW cell. RAW cells were incubated with both 5 μM ApoB-GFP and 5 μg mL^{-1} FM 4-64 for 3 h. Fluorescence images of cells were acquired by confocal microscopy with a 100× oil immersion objective (Plan-Neofluar 100×, Carl Zeiss). The fluorescence images shows colocalization of ApoB-GFP and endosomal vesicles stained with FM 4-64. Scale bar represents 10 μm.

result indicates that ApoB-GFP is in fact incorporated into RAW cells through an endocytotic pathway after binding with SR-AI.

We next describe the inhibitory domain of the present probe. Trigger factor (TF) is a chaperon protein (*19*) derived from *Escherichia coli* with a molecular weight 2-fold larger than that of $ApoB_{547-735}$ (TF, 48 kDa; $ApoB_{547-735}$, 21 kDa). We expected that TF would block the interaction be-tween $ApoB_{547-735}$ and SR-AI by steric hindrance when $ApoB_{547-735}$ is fused with TF. The fusion of TF with the N-terminus of the $ApoB_{547-735}$ domain (termed TF-ApoB-GFP, Figure 1, panel c) resulted in a complete loss of the green fluorescence within RAW cells, as expected (Figure 4, panels a and b). This result indicates that the TF domain of TF-ApoB-GFP inhibits the interaction between the $ApoB_{547-735}$ domain and SR-AI. We thus constructed the present targeting-probe, TF-M-ApoB-GFP, using TF and $ApoB_{547-735}$. We inserted the MMP-9 cleavable linker sequence, Val-Pro-Leu-Ser-Leu-Tyr-Ser-Gly (*20*), between the TF domain and the $ApoB_{547-735}$ domain so that the $ApoB_{547-735}$ domain is exposed when the cleavable linker is digested by MMP-9.

We examined whether MMP-9 digests the cleavable linker inserted between the TF domain and the $ApoB_{547-735}$ domain. We mixed TF-M-ApoB-GFP with various concentrations of the activated form of MMP-9 in a cell-free system, and allowed the mixture to incubate for 2 h at 37 °C. The samples were examined by immunoblot analysis with anti-GFP antibody (Figure 4, panel c). Upon treatment of TF-M-ApoB-GFP with the activated form of MMP-9, two bands appeared corresponding to intact TF-M-ApoB-GFP and a cleaved product of TF-M-ApoB-GFP. TF-M-ApoB-GFP was cleaved in an MMP-9-dependent fashion (Figure 4, panel d). The result shows that the TF domain of TF-M-ApoB-GFP is actually removable upon its cleavage by the activated form of MMP-9.

We added TF-M-ApoB-GFP treated or untreated with the activated form of MMP-9 to RAW cells (Figure 4, panels e and f). TF-M-ApoB-GFP precleaved with MMP-9 was incorporated into RAW cells, whereas uncleaved TF-M-ApoB-GFP was not incorporated into RAW cells. This shows that the present fluorescent targeting probe, TF-M-ApoB-GFP, is incorporated into macrophages only when the TF domain is cleaved by MMP-9.

We next examined whether TF-M-ApoB-GFP targets macrophages expressing both SR-AI and the activated form of MMP-9. We expressed an autoactivating form of MMP-9 (MMP-9-G100L) in RAW cells. This is because RAW cells express SR-AI but do not express the activated form of MMP-9 to a large extent. When we added TF-M-ApoB-

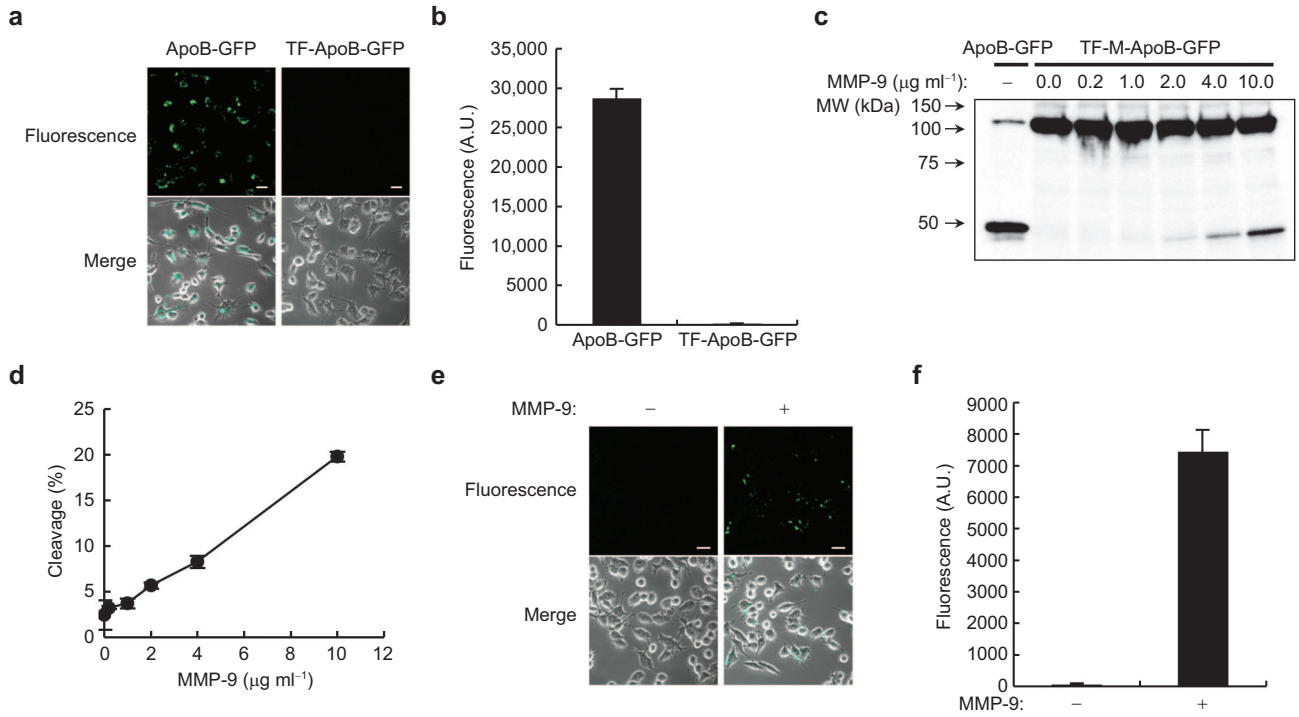

Figure 4. The present fluorescent targeting probe is incorporated into macrophages upon cleavage by MMP-9. a, b) RAW cells incubated with 1 μM ApoB-GFP or with 1 μM TF-ApoB-GFP for 3 h and then observed by confocal microscopy with a 40× objective. a) Typical experiments from three independent measurements. Scale bar represents 20 μm. b) Green fluorescence intensities inside the cells in panel a. Error bars represent standard deviation ($n = 3$). c, d) MMP-9-dependent cleavage of the present targeting probe. TF-M-ApoB-GFP (1 μM) was incubated with various concentrations of the activated form of MMP-9 for 2 h at 37 °C and subjected to imunnoblotting analysis with anti-GFP antibody (panel c). ApoB-GFP was also subjected to imunnoblotting analysis as a control (panel c). The blot shown in panel c is representative of three separate experiments. Percentage cleavage was calculated from two band densities in panel c, that is, the upper band (97 kDa) corresponding to intact TF-M-ApoB-GFP and the lower band (49 kDa) corresponding to a cleaved product of TF-M-ApoB-GFP. Panel d shows the average of three independent trials. Error bars indicate standard deviation. e, f) TF-M-ApoB-GFP (1 μM) incubated with 10 μg mL^{-1} MMP-9 for 2 h at 37 °C and then added to RAW cells. After a 3 h incubation, fluorescence images were acquired by confocal microscopy with a 40× objective. e) Typical experiments from three independent measurements. Scale bar represents 20 μm. f) Green fluorescence intensities inside the cells in panel e. Error bars represent standard deviation of three independent experiments.

GFP to the cells, an apparent increase in the green fluorescence was observed within the cells (Figure 5, panels a and b). While we added TF-M-ApoB-GFP to RAW cells expressing control vector, no significant green fluorescence was detected within the cells. The result demonstrates that the incorporation of the probe into macrophage-like RAW cells is synergistically activated by SR-AI and MMP-9.

To show selective targeting of activated macrophages by TF-M-ApoB-GFP, we cocultured the RAW cells expressing MMP-9-G100L with vascular endothelial cells. Prior to the coculture, we stained the vascular endothelial cells with PKH26, a cell membrane labeling agent, to distinguish the RAW cells from the endothelial cells. We then added TF-M-ApoB-GFP to the cocultured RAW cells expressing MMP-9-G100L and the endothelial cells. The green fluorescence of the present targeting probe was observed only in the RAW cells but not in the endothelial cells that express neither SR-AI nor MMP-9 (Figure 5, panel c). This result shows that TF-M-ApoB-GFP allows selective targeting of macrophage-like RAW cells having both SR-AI and MMP-9, without its wrong incorporation into neighboring cells expressing neither SR-AI nor MMP-9, such as vascular endothelial cells.

We further examined the uptake of the present probe by authentic human cells, such as monocytes, resting macrophages, and activated macrophages (Figure 6). Human peripheral blood monocytes, which do not express both SR-AI and MMP-9, exhibited no detectable incorporation of the present fluorescent targeting probe. Also,

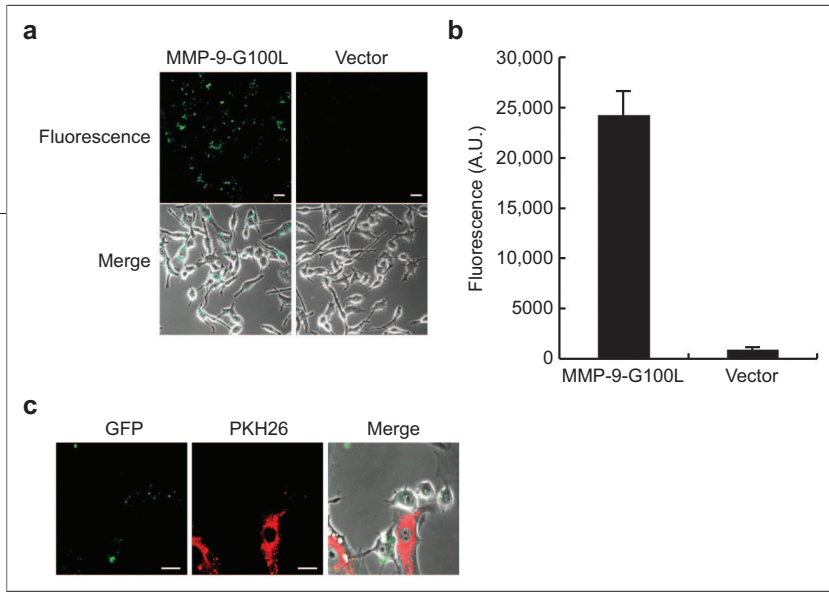

Figure 5. The incorporation of the present fluorescent targeting probe into macrophages is synergistically activated by SR-AI and an activated form of MMP-9. a, b) RAW cells having SR-AI transfected with MMP-9-G100L or control vector for 24 h. The cells were incubated with 2 μM TF-M-ApoB-GFP for 3 h, and then fluorescence images were acquired by confocal microscopy with a 40× objective. a) Typical experiments from three independent measurements. Scale bar represents 20 μm. b) Green fluorescence intensities inside the cells in panel a. Error bars represent standard deviation of three independent experiments. c) Selective targeting by TF-M-ApoB-GFP of macrophages cocultured with vascular endothelial cells. RAW cells expressing both SR-AI and MMP-9-G100L were cocultured with vascular endothelial cells stained with PKH26. The cocultured cells were incubated with 2 μM TF-M-ApoB-GFP for 3 h, and then fluorescence images were acquired by confocal microscopy with a 40× objective. Scale bar represents 20 μm.

human resting macrophages, which express only SR-AI but not the activated form of MMP-9, did not incorporate the probe. To obtain activated macrophages, we stimulated resting macrophages with lipopolysaccharide (LPS) for 24 h. When we added TF-M-ApoB-GFP to the activated macrophages, the significant increase in the green fluorescence was observed within the cells. The result shows that TF-M-ApoB-GFP provides a powerful tool for selective targeting of human activated macrophages.

TF-M-ApoB-GFP having GFP for the reporter domain allowed the detection of single macrophages with fluorescence readout as shown above. We next show that the reporter domain of the present probe can be customized. Bioluminescent proteins, luciferases, allow autofluorescence-free and highly sensitive bioanalysis (*21*, *22*). We replaced the GFP domain of ApoB-GFP with luciferase derived from *Renilla reniformis* (rLuc), and named the resulting construct ApoB-rLuc (Figure 1, panel c). We incubated ApoB-rLuc with RAW cells in the absence or presence of polyinosinic acid that inhibits the SR-AI-mediated endocytotic pathway. We found that the bioluminescence intensity of ApoB-rLuc from the cells increases in a dose-dependent fashion in the absence of polyinosinic acid but not in the presence of polyinosinic acid (Figure 7, panel a). The net bioluminescence of ApoB-rLuc incorporated into the RAW cells exhibited a proportional increase to the concentration of ApoB-rLuc (Figure 7, panel b). The result shows that ApoB-rLuc is incorporated into macrophages through the SR-AI-mediated endocytotic pathway, as well as ApoB-GFP.

We next generated TF-M-ApoB-rLuc by replacing the GFP domain of TF-M-ApoB-GFP with rLuc (Figure 1, panel c). We examined whether TF-M-ApoB-rLuc targets macrophages expressing both SR-AI and the activated form of MMP-9. When we added TF-M-ApoB-rLuc to RAW cells expressing MMP-9-G100L, bioluminescence signals were observed from the cells in a dose-dependent fashion (Figure 7, panel c). On the other hand, RAW cells expressing control vectors exhibited no significant bioluminescence signals. The result demonstrates that, in addition to TF-M-ApoB-GFP, TF-M-ApoB-rLuc targets the cells having SR-AI and the activated form of MMP-9. This shows that the reporter domain of the present probe is in fact flexibly customizable.

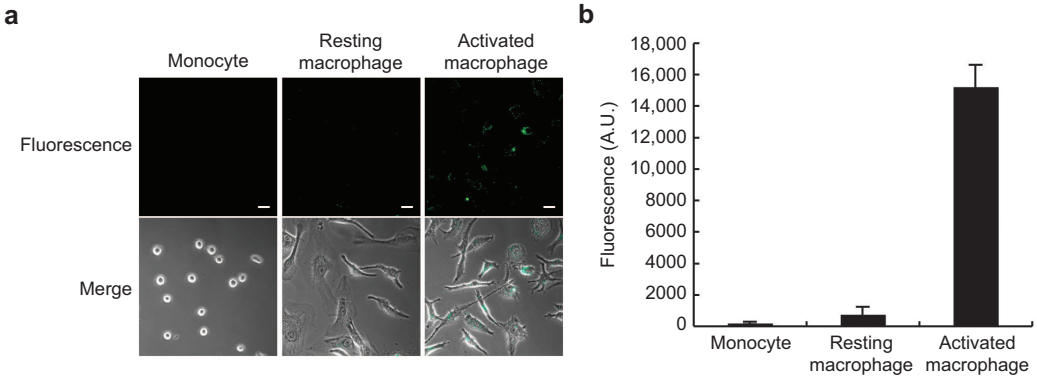

Figure 6. The present fluorescent targeting probe allows selective targeting of human activated macrophages. a, b) Human peripheral blood monocytes, resting macrophages, and LPS-activated macrophages were incubated with 2 μM TF-M-ApoB-GFP for 3 h, and then fluorescence images were observed by confocal microscopy with a 40× objective. a) Typical experiments from three independent measurements. Scale bar represents 20 μm. b) Green fluorescence intensities inside the cells in panel a. Error bars represent standard deviation of three independent experiments.

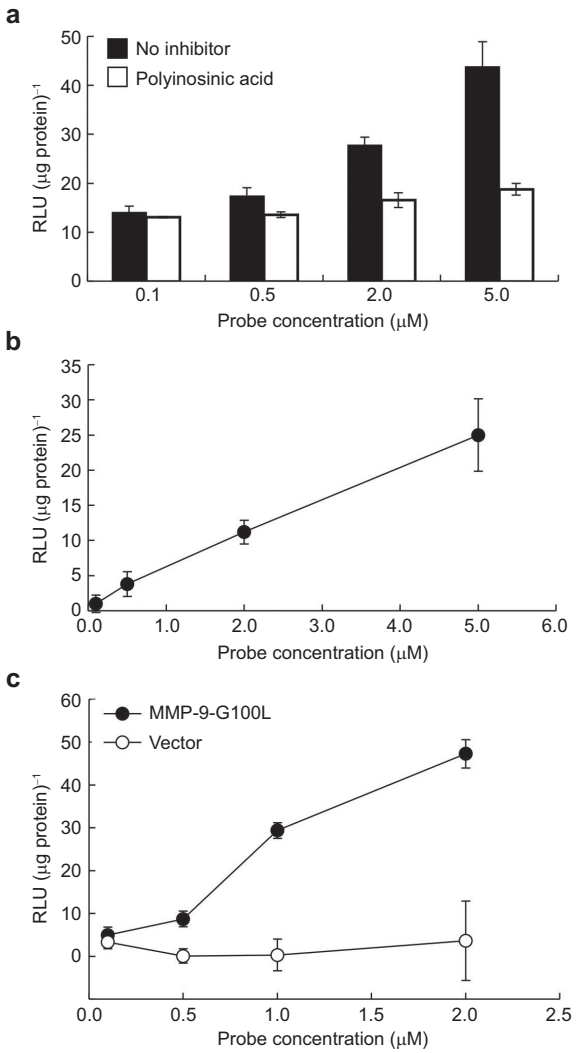

Figure 7. The reporter domain of the present targeting probe can be customized. a) RAW cells were incubated with indicated concentrations of ApoB-rLuc in the presence or absence of 1 mg mL^{-1} of polyinosinic acid. The bioluminescence intensities were normalized by protein concentrations of each well (mean ± standard error of the mean, $n \geq 3$). b) Net bioluminescence from ApoB-rLuc incorporated into RAW cells. c) TF-M-ApoB-rLuc selectively targets macrophages that express the activated form of MMP-9, MMP-9-G100L. RAW cells were transfected with MMP-9-G100L or control vector for 24 h and incubated with indicated concentrations of TF-M-ApoB-rLuc for 3 h. Net bioluminescence intensities were shown (mean ± standard error of the mean, $n \geq 3$).

Finally, we examined whether the present targeting probes, including TF-M-ApoB-GFP and TF-M-ApoB-rLuc, exerts toxic effects on macrophages. As shown in Figure 8, the present targeting probes do not affect the viability of macrophages, regardless whether or not the expression of the activated form of MMP-9 is enhanced. This shows that the incorporation of the present probes has no toxic effects on macrophages.

DISCUSSION

In the present study, we have developed a method for the selective targeting of activated macrophages. We have shown that the core-binding domain of ApoB ($ApoB_{547-735}$) binds to SR-AI but not to other SR isoforms, SR-BI and CD36, whereas oxLDL that contains the full length of ApoB binds to SR-AI, SR-BI, and CD36. We used the SR-AI-selective $ApoB_{547-735}$, but not the full-length of ApoB, for the receptor-binding domain of the present targeting probes. This is advantageous for targeting macrophages because SR-AI is predominantly expressed in macrophages (*18*). In contrast, SR-BI is highly expressed in the liver, as well as steroidogenic tissues such as the adrenal glands, ovaries, and testes (*8*). Also, CD36 has a wide tissue distribution, including monocytes, adipocytes, microvascular endothelium, platelets, and erythroid precursors (*8*). However, the SR-AI-selective binding of $ApoB_{547-735}$ is still not sufficient to selectively target activated macrophages because SR-AI is expressed not only in activated macrophages but also in resting macrophages in normal tissues, such as liver, kidney, and lung (*8, 9*). We then took notice of the fact that activated macrophages coexpress SR-AI and the activated form of MMP-9 (*10, 12, 13*), different from resting macrophages in normal tissues. We have thus designed the present targeting probes, TF-M-ApoB-GFP and TF-M-ApoB-rLuc, to be uncaged by MMP-9 and then to bind to SR-AI. We demonstrated that the present targeting probes are incorporated into macrophages having SR-AI and the activated form of MMP-9, which are the marker receptor and protease of atherosclerotic lesions, respectively.

We further demonstrated that the present targeting probes are exclusively incorporated into macrophages having both SR-AI and the activated form of MMP-9, without wrong incorporation into neighboring endothelial cells that do not have SR-AI. Tsien's group previously developed polyarginine-based imaging probes, which are incorporated into cells after their cleavage by MMPs (*23*). However, once the polyarginine-based imaging probes are cleaved by MMPs, the cleaved probes are nonspecifically incorporated into any cell types, including disease cells and healthy cells (*24*). Our results show that the present probe, of which uptake is synergistically activated by the marker receptor SR-AI and the marker protease MMP-9, is superior to the previous MMP-cleavable probes in terms of the selectivity to particular cell types, including activated macrophages.

We also demonstrated that the reporter domain of the present probe can be customized. Red fluorescent proteins (*25*) have recently been developed and used for *in vivo* imaging because their near-infrared fluorescence is highly tissue-transparent. The red

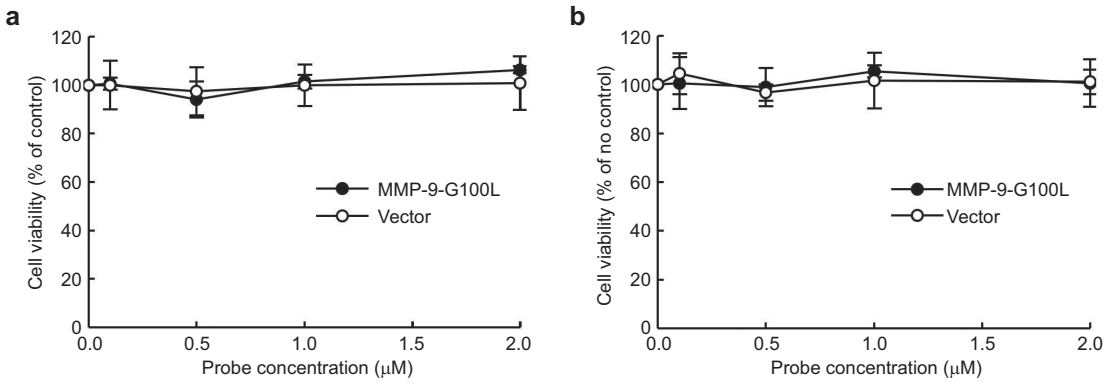

Figure 8. Cell viability. a, b) RAW cells transfected with MMP-9-G100L or control vectors were incubated with indicated concentrations of TF-M-ApoB-GFP (panel a) or TF-M-ApoB-rLuc (panel b) for 3 h and then measured the cell viability by tripan blue exclusion assay. Error bars represent standard deviation ($n = 3$).

fluorescent proteins may be ideal for the reporter domain of the present probe for imaging of disease cells in deep tissues in living animals. Luciferases, such as rLuc and red-shifted rLuc variants (*26*), may also be useful reporters to detect disease cells in living animals because these reporters allow autofluorescence-free and highly sensitive imaging *in vivo*. In addition to imaging of disease cells, therapeutic applications may be possible by replacing the reporter domain of the present probe with biologically active proteins, which suppress aberrant cellular signaling of disease cells (*27*) or induce cell death (*28*).

METHODS

Materials. Polyinosinic acid, LPS, and PKH26 were purchased from Sigma Chemical Co. (St. Louis, MO). DiI-acLDL and CTB-Alexa 647 were obtained from Molecular Probes Inc. (Eugene, OR). Human recombinant active MMP-9 was purchased from Novagen (Madison, WI). Other chemicals were purchased from Wako Pure Chemical Industries (Osaka, Japan). Human peripheral blood $CD14^+$ monocytes were obtained from Lonza Group Ltd. (Basel, Switzerland). Expression vectors encoding SR-AI, SR-BI, and CD36 were kindly gifted by Dr. Hiroyuki Arai (the University of Tokyo). A cDNA encoding MMP-9 was kindly gifted by Dr. Hiroshi Sato (Kanazawa University).

Plasmid Construction. To construct expression plasmids encoding the present probes, fragment cDNAs encoding a peptide segment of apolipoprotein B ($ApoB_{547-735}$), $ApoB_{547-735}$ with MMP-9 cleavable linker, green fluorescent protein (GFP) with a flexible linker, and *Renilla reniformis* luciferase (rLuc) with the flexible linker were generated by PCR. The cDNA encoding ApoB-GFP, ApoB-rLuc, TF-M-ApoB-GFP, and TF-M-ApoB-rLuc were generated by fusing the fragment cDNA of $ApoB_{547-735}$ or $ApoB_{547-735}$ with MMP-9 cleavable linker to the fragment cDNA of GFP or rLuc in pCold TF DNA vector (Takara Bio Inc., Shiga, Japan). All cloning enzymes were from Takara Bio Inc. (Shiga, Japan) and were used according to the manufacturer's instructions. All PCR fragments were sequenced with an ABI310 genetic analyzer.

Protein Expression and Purification. Expression plasmids encoding ApoB-GFP, ApoB-rLuc, TF-M-ApoB-GFP, and TF-M-ApoB-rLuc were transformed into BL21 (DE3) pLysS (Novagen, Madison, WI) competent cells. Expression of the probes was induced with 0.5 mM of isopropyl β-$_D$-1-thiogalactopyranoside for 20 h at 15 °C. Each probe having a His-tag was purified with a TALON CellThru resin (Clontech, Mountain View, CA). The purified probes were dialyzed against a buffer containing 25 mM of HEPES (pH 7.5) overnight at 4 °C. ApoB-GFP and ApoB-rLuc were further treated with HRV 3C protease (Novagen, Madison, WI) and again purified with the TALON CellThru resin. Protein concentration was determined using a Bio-Rad Protein Assay (Bio-Rad Laboratories, Hercules, CA) based on the method of Bradford. We kept all of the purified proteins at −80 °C until use.

Cell Culture. Chinese hamster ovary (CHO-K1) cells were cultured in Ham's F-12 medium supplemented with 10% fetal calf serum (FCS) at 37 °C in 5% CO_2. RAW 264.7 mouse macrophages were cultured in Dulbecco's modified Eagle's medium (Gibco, Grand Island, NY) supplemented with 10% FCS and 4 mM L-glutamine at 37 °C in 5% CO_2. Vascular endothelial cells derived from bovine pulmonary artery (CPAE cells) were cultured in Eagle's minimum essential medium supplemented with 20% FCS, 1% penicillin/streptomycin, 1 mM sodium pyruvate, and 0.1 mM nonessential amino acids at 37 °C in 5% CO_2. Human peripheral blood $CD14^+$ monocytes were cultured in hematopoietic progenitor growth medium (HPGM, Lonza Group Ltd.) supplemented with 10% FCS. To differentiate to macrophages, the monocytes were cultured in HPGM in the absence of FCS for 7 days.

Microscopy. CHO-K1 cells or RAW cells were incubated with ApoB-GFP for 3 h at 37 °C in 5% CO_2. The present probes were prepared with phenol red-free DMEM (Gibco, Grand Island, NY) containing 10% FCS to avoid the autofluorescence from phenol red in our experimental tests. The cells were washed and immersed in Hanks' balanced salt solution. Fluorescence images were acquired using a confocal laser scanning microscope (LSM 510, Carl Zeiss) at RT.

Immunoblotting Analysis. The sample was separated by SDS-PAGE and electrophoretically transferred onto a nitrocellulose membrane. The membrane was detected with anti-GFP antibody (Living Colors A.v. Peptide Antibody, Clontech, Mountain View, CA) and then with peroxidase-labeled ECL antirabbit IgG antibody (Amersham Biosciences, Piscataway, NJ). The secondary antibody was visualized with ECL Western Blotting Detection Reagents (Amersham Biosciences, Piscataway, NJ) by using a LAS-1000 plus image analyzer (Fuji Film Co., Tokyo, Japan). Band densities were measured by using an image analysis software Multi Gauge Ver.3.X (Fuji Film Co.). The percentage of MMP-9-dependent cleavage of the present targeting probe was calculated as the following formula; cleavage (%) = 49 kDa band density/(97 kDa band density + 49 kDa band density) × 100.

Bioluminescence Assay. RAW cells were plated onto 24-well microplates and incubated with various concentrations of ApoB-rLuc or TF-M-ApoB-rLuc for 3 h at 37 °C in 5% CO_2. To remove nonspecific binding of the present probes to cell surface and microplate, we trypsinized the RAW cells and collected the cells by centrifugation at 1800*g* for 3 min. Cell pellet was resuspended with 20 μL of PBS. We then added 80 μL of cell lysis buffer to the sample. The mixture was incubated for 15 min at RT, and 20 μL of the mixture was assayed with 100 μL of Renilla Luciferase Assay Reagent (Promega Co., Madison, WI) containing coelenterazine (Promega Co.) as a substrate. The bioluminescence of the incorporated probes was measured for first 10 s with a Minilumat LB9506 luminometer (Berthold GmbH & Co. KG, Wildbad, Germany).

The bioluminescence intensity was normalized against the protein concentration of each well.

Cell Viability. Cells were collected by trypsinization and resuspended in 90 μL of PBS. Ten microliters of 0.4% trypan blue solution was then added to the resuspended cells. The numbers of live cells that were not stained with trypan blue were counted in a hemocytometer.

Acknowledgment: This work was supported by the Japan Society for the Promotion of Science (JSPS), the Takeda Science Foundation (to M.S.), and the Global COE Program for Chemistry Innovation.

REFERENCES

1. Garnett, M. C. (2001) Targeted drug conjugates: principles and progress, *Adv. Drug Delivery Rev. 53*, 171–216.
2. Juliano, R. (2007) Challenges to macromolecular drug delivery, *Biochem. Soc. Trans. 35*, 41–43.
3. Wickline, S. A., and Lanza, G. M. (2003) Nanotechnology for molecular imaging and targeted therapy, *Circulation 107*, 1092–1095.
4. Huh, Y. M., Jun, Y. W., Song, H. T., Kim, S., Choi, J. S., Lee, J. H., Yoon, S., Kim, K. S., Shin, J. S., Suh, J. S., and Cheon, J. (2005) In vivo magnetic resonance detection of cancer by using multifunctional magnetic nanocrystals, *J. Am. Chem. Soc. 127*, 12387–12391.
5. Shadidi, M., and Sioud, M. (2003) Selective targeting of cancer cells using synthetic peptides, *Drug Resist. Updates 6*, 363–371.
6. Toublan, F. J. J., Boppart, S., and Suslick, K. S. (2006) Tumor targeting by surface-modified protein microspheres, *J. Am. Chem. Soc. 128*, 3472–3473.
7. Li, A. C., and Glass, C. K. (2002) The macrophage foam cell as a target for therapeutic intervention, *Nat. Med. 8*, 1235–1242.
8. Murphy, J. E., Tedbury, P. R., Homer-Vanniasinkam, S., Walker, J. H., and Ponnambalam, S. (2005) Biochemistry and cell biology of mammalian scavenger receptors, *Atherosclerosis 182*, 1–15.
9. Tomokiyo, R., Jinnouchi, K., Honda, M., Wada, Y., Hanada, N., Hiraoka, T., Suzuki, H., Kodama, T., Takahashi, K., and Takeya, M. (2002) Production, characterization, and interspecies reactivities of monoclonal antibodies against human class A macrophage scavenger receptors, *Atherosclerosis 161*, 123–132.
10. Loftus, I. M., Naylor, A. R., Goodall, S., Crowther, M., Jones, L., Bell, P. R. F., Thompson, M. M., and Thompson, M. (2000) Increased matrix metalloproteinase-9 activity in unstable carotid plaques A potential role in acute plaque disruption, *Stroke 31*, 40–47.
11. Galis, Z. S., and Khatri, J. J. (2002) Matrix metalloproteinases in vascular remodeling and atherogenesis: the good, the bad, and the ugly, *Circ. Res. 90*, 251–262.
12. Brown, D. L., Hibbs, M. S., Kearney, M., Loushin, C., and Isner, J. M. (1995) Identification of 92-kD gelatinase in human coronary atherosclerotic lesions: association of active enzyme-synthesis with unstable angina, *Circulation 91*, 2125–2131.
13. Gough, P. J., Gomez, I. G., Wille, P. T., and Raines, E. W. (2006) Macrophage expression of active MMP-9 induces acute plaque disruption in apoE-deficient mice, *J. Clin. Invest. 116*, 59–69.
14. Segrest, J. P., Jones, M. K., De Loof, H., and Dashti, N. (2001) Structure of apolipoprotein B-100 in low density lipoproteins, *J. Lipid Res. 42*, 1346–1367.
15. Parthasarathy, S., Fong, L. G., Otero, D., and Steinberg, D. (1987) Recognition of solubilized apoproteins from delipidated, oxidized low-density-lipoprotein (LDL) by the acetyl-LDL receptor, *Proc. Natl. Acad. Sci. U.S.A. 84*, 537–540.
16. Bird, D. A., Gillotte, K. L., Horkko, S., Friedman, P., Dennis, E. A., Witztum, J. L., and Steinberg, D. (1999) Receptors for oxidized low-density lipoprotein on elicited mouse peritoneal macrophages can recognize both the modified lipid moieties and the modified protein moieties: implications with respect to macrophage recognition of apoptotic cells, *Proc. Natl. Acad. Sci. U.S.A. 96*, 6347–6352.
17. Kreuzer, J., White, A. L., Knott, T. J., Jien, M. L., Mehrabian, M., Scott, J., Young, S. G., and Haberland, M. E. (1997) Amino terminus of apolipoprotein B suffices to produce recognition of malondialdehyde-modified low density lipoprotein by the scavenger receptor of human monocyte-macrophages, *J. Lipid Res. 38*, 324–342.
18. Moore, K. J., and Freeman, M. W. (2006) Scavenger receptors in atherosclerosis: beyond lipid uptake, *Arterioscler., Thromb., Vasc. Biol. 26*, 1702–1711.
19. Hartl, F. U., and Hayer-Hartl, M. (2002) Molecular chaperones in the cytosol: from nascent chain to folded protein, *Science 295*, 1852–1858.
20. Turk, B. E., Huang, L. L., Piro, E. T., and Cantley, L. C. (2001) Determination of protease cleavage site motifs using mixture-based oriented peptide libraries, *Nat. Biotechnol. 19*, 661–667.
21. Fan, F., and Wood, K. V. (2007) Bioluminescent assays for high-throughput screening, *Assay Drug Dev. Technol. 5*, 127–136.
22. Contag, P. R., Olomu, I. N., Stevenson, D. K., and Contag, C. H. (1998) Bioluminescent indicators in living mammals, *Nat. Med. 4*, 245–247.
23. Jiang, T., Olson, E. S., Nguyen, Q. T., Roy, M., Jennings, P. A., and Tsien, R. Y. (2004) Tumor imaging by means of proteolytic activation of cell-penetrating peptides, *Proc. Natl. Acad. Sci. U.S.A. 101*, 17867–17872.
24. Zorko, M., and Langel, U. (2005) Cell-penetrating peptides: mechanism and kinetics of cargo delivery, *Adv. Drug Delivery Rev. 57*, 529–545.
25. Shcherbo, D., Merzlyak, E. M., Chepurnykh, T. V., Fradkov, A. F., Ermakova, G. V., Solovieva, E. A., Lukyanov, K. A., Bogdanova, E. A., Zaraisky, A. G., Lukyanov, S., and Chudakov, D. M. (2007) Bright far-red fluorescent protein for whole-body imaging, *Nat. Methods 4*, 741–746.
26. Loening, A. M., Wu, A. M., and Gambhir, S. S. (2007) Red-shifted Renilla reniformis luciferase variants for imaging in living subjects, *Nat. Methods 4*, 641–643.
27. Borsello, T., Clarke, P. G. H., Hirt, L., Vercelli, A., Repici, M., Schorderet, D. F., Bogousslavsky, J., and Bonny, C. (2003) A peptide inhibitor of c-Jun N-terminal kinase protects against excitotoxicity and cerebral ischemia, *Nat. Med. 9*, 1180–1186.
28. Vocero-Akbani, A. M., Vander Heyden, N., Lissy, N. A., Ratner, L., and Dowdy, S. F. (1999) Killing HIV-infected cells by transduction with an HIV protease-activated caspase-3 protein, *Nat. Med. 5*, 29–33.